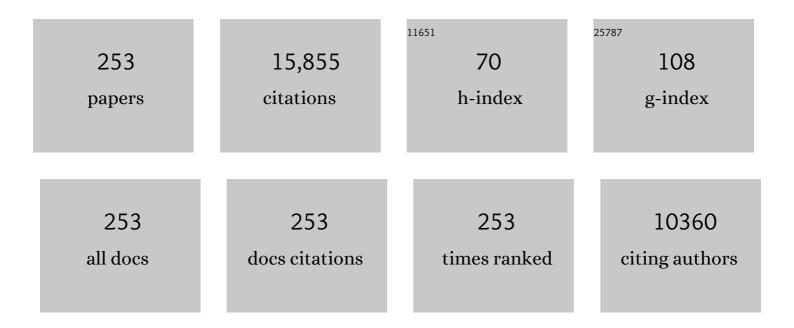
List of Publications by Year in descending order

Source: https://exaly.com/author-pdf/1569118/publications.pdf Version: 2024-02-01



#	Article	IF	CITATIONS
1	A critical review of extracellular polymeric substances (EPSs) in membrane bioreactors: Characteristics, roles in membrane fouling and control strategies. Journal of Membrane Science, 2014, 460, 110-125.	8.2	583
2	A review on anaerobic membrane bioreactors: Applications, membrane fouling and future perspectives. Desalination, 2013, 314, 169-188.	8.2	545
3	Membrane Bioreactors for Industrial Wastewater Treatment: A Critical Review. Critical Reviews in Environmental Science and Technology, 2012, 42, 677-740.	12.8	256
4	In situ preparation of g-C3N4/Bi4O5I2 complex and its elevated photoactivity in Methyl Orange degradation under visible light. Journal of Environmental Sciences, 2020, 87, 149-162.	6.1	227
5	Efficient degradation of RhB over GdVO4/g-C3N4 composites under visible-light irradiation. Chemical Engineering Journal, 2013, 215-216, 721-730.	12.7	219
6	Membrane fouling in a membrane bioreactor: High filtration resistance of gel layer and its underlying mechanism. Water Research, 2016, 102, 82-89.	11.3	209
7	Enhanced photodegradation activity of methyl orange over Z-scheme type MoO <sub>3</sub> –g-C <sub>3</sub> N <sub>4</sub> composite under visible light irradiation. RSC Advances, 2014, 4, 13610-13619.	3.6	205
8	A unified thermodynamic mechanism underlying fouling behaviors of soluble microbial products (SMPs) in a membrane bioreactor. Water Research, 2019, 149, 477-487.	11.3	203
9	Microwave heating preparation of phosphorus doped g-C3N4 and its enhanced performance for photocatalytic H2 evolution in the help of Ag3PO4 nanoparticles. International Journal of Hydrogen Energy, 2020, 45, 14354-14367.	7.1	195
10	Synergistic fouling behaviors and mechanisms of calcium ions and polyaluminum chloride associated with alginate solution in coagulation-ultrafiltration (UF) process. Water Research, 2021, 189, 116665.	11.3	191
11	Membrane fouling caused by biological foams in a submerged membrane bioreactor: Mechanism insights. Water Research, 2020, 181, 115932.	11.3	189
12	New insights into membrane fouling in a submerged anaerobic membrane bioreactor based on characterization of cake sludge and bulk sludge. Bioresource Technology, 2011, 102, 2373-2379.	9.6	176
13	New methods based on back propagation (BP) and radial basis function (RBF) artificial neural networks (ANNs) for predicting the occurrence of haloketones in tap water. Science of the Total Environment, 2021, 772, 145534.	8.0	176
14	In-situ synthesis of AgNbO3/g-C3N4 photocatalyst via microwave heating method for efficiently photocatalytic H2 generation. Journal of Colloid and Interface Science, 2019, 534, 163-171.	9.4	174
15	Fabrication of high-performance composite nanofiltration membranes for dye wastewater treatment: mussel-inspired layer-by-layer self-assembly. Journal of Colloid and Interface Science, 2020, 560, 273-283.	9.4	170
16	Mechanistic insights into alginate fouling caused by calcium ions based on terahertz time-domain spectra analyses and DFT calculations. Water Research, 2018, 129, 337-346.	11.3	168
17	Facile fabrication of novel Ag2S/K-g-C3N4 composite and its enhanced performance in photocatalytic H2 evolution. Journal of Colloid and Interface Science, 2020, 568, 117-129.	9.4	167
18	Synthesis of carbon-doped KNbO3 photocatalyst with excellent performance for photocatalytic hydrogen production. Solar Energy Materials and Solar Cells, 2018, 179, 45-56.	6.2	163

#	Article	IF	CITATIONS
19	Feasibility evaluation of submerged anaerobic membrane bioreactor for municipal secondary wastewater treatment. Desalination, 2011, 280, 120-126.	8.2	160
20	A high-performance hybrid supercapacitor with NiO derived NiO@Ni-MOF composite electrodes. Electrochimica Acta, 2020, 340, 135956.	5.2	157
21	NMR-based metabonomic study of the sub-acute toxicity of titanium dioxide nanoparticles in rats after oral administration. Nanotechnology, 2010, 21, 125105.	2.6	154
22	Facile synthesis of 2D TiO2@MXene composite membrane with enhanced separation and antifouling performance. Journal of Membrane Science, 2021, 640, 119854.	8.2	154
23	Inkjet printing of dopamine followed by UV light irradiation to modify mussel-inspired PVDF membrane for efficient oil-water separation. Journal of Membrane Science, 2021, 619, 118790.	8.2	149
24	Molecular Engineering toward Pyrrolic Nâ€Rich Mâ€N <sub>4</sub> (M = Cr, Mn, Fe, Co, Cu) Singleâ€Atom Sites for Enhanced Heterogeneous Fenton‣ike Reaction. Advanced Functional Materials, 2021, 31, 2007877.	14.9	139
25	Comparing Two New Composite Photocatalysts, <i>t</i> -LaVO <sub>4</sub> /g-C <sub>3</sub> N <sub>4</sub> and <i>m</i> -LaVO <sub>4</sub> /g-C <sub>3</sub> N <sub>4</sub> , for Their Structures and Performances. Industrial & amp: Engineering Chemistry Research, 2014, 53, 5905-5915.	3.7	137
26	Rapid and energy-efficient preparation of boron doped g-C3N4 with excellent performance in photocatalytic H2-evolution. International Journal of Hydrogen Energy, 2018, 43, 19984-19989.	7.1	137
27	Fouling mechanisms of gel layer in a submerged membrane bioreactor. Bioresource Technology, 2014, 166, 295-302.	9.6	133
28	Factors affecting THMs, HAAs and HNMs formation of Jin Lan Reservoir water exposed to chlorine and monochloramine. Science of the Total Environment, 2013, 444, 196-204.	8.0	131
29	Effect of calcium ions on fouling properties of alginate solution and its mechanisms. Journal of Membrane Science, 2017, 525, 320-329.	8.2	131
30	Effects of hydrophilicity/hydrophobicity of membrane on membrane fouling in a submerged membrane bioreactor. Bioresource Technology, 2015, 175, 59-67.	9.6	130
31	Enhanced permeability and antifouling performance of polyether sulfone (PES) membrane via elevating magnetic Ni@MXene nanoparticles to upper layer in phase inversion process. Journal of Membrane Science, 2021, 623, 119080.	8.2	130
32	Synthesis and characterization of a ZrO <sub>2</sub> /g-C <sub>3</sub> N <sub>4</sub> composite with enhanced visible-light photoactivity for rhodamine degradation. RSC Advances, 2014, 4, 40029-40035.	3.6	121
33	A new insight into membrane fouling mechanism in submerged membrane bioreactor: Osmotic pressure during cake layer filtration. Water Research, 2013, 47, 2777-2786.	11.3	117
34	Efficient degradation and mineralization of antibiotics via heterogeneous activation of peroxymonosulfate by using graphene supported single-atom Cu catalyst. Chemical Engineering Journal, 2020, 394, 124904.	12.7	117
35	Different fouling propensities of loosely and tightly bound extracellular polymeric substances (EPSs) and the related fouling mechanisms in a membrane bioreactor. Chemosphere, 2020, 255, 126953.	8.2	112
36	A novel Bi <sub>2</sub> S <sub>3</sub> /KTa <sub>0.75</sub> Nb <sub>0.25</sub> O <sub>3</sub> nanocomposite with high efficiency for photocatalytic and piezocatalytic N <sub>2</sub> fixation. Journal of Materials Chemistry A, 2021, 9, 13344-13354.	10.3	109

#	Article	IF	CITATIONS
37	Preparation of Ni@UiO-66 incorporated polyethersulfone (PES) membrane by magnetic field assisted strategy to improve permeability and photocatalytic self-cleaning ability. Journal of Colloid and Interface Science, 2022, 618, 483-495.	9.4	109
38	A conductive PVDF-Ni membrane with superior rejection, permeance and antifouling ability via electric assisted in-situ aeration for dye separation. Journal of Membrane Science, 2019, 581, 401-412.	8.2	107
39	Prediction of interfacial interactions related with membrane fouling in a membrane bioreactor based on radial basis function artificial neural network (ANN). Bioresource Technology, 2019, 282, 262-268.	9.6	105
40	Magnetic field assisted arrangement of photocatalytic TiO2 particles on membrane surface to enhance membrane antifouling performance for water treatment. Journal of Colloid and Interface Science, 2020, 570, 273-285.	9.4	105
41	Fabrication and characterization of hollow CdMoO4 coupled g-C3N4 heterojunction with enhanced photocatalytic activity. Journal of Hazardous Materials, 2015, 299, 333-342.	12.4	104
42	Metal-phenolic network as precursor for fabrication of metal-organic framework (MOF) nanofiltration membrane for efficient desalination. Journal of Membrane Science, 2021, 624, 119101.	8.2	104
43	In-situ preparation of Z-scheme AgI/Bi5O7I hybrid and its excellent photocatalytic activity. Applied Surface Science, 2016, 387, 912-920.	6.1	101
44	Rapid fabrication of KTa0.75Nb0.25/g-C3N4 composite via microwave heating for efficient photocatalytic H2 evolution. Fuel, 2019, 241, 1-11.	6.4	101
45	A novel in-situ micro-aeration functional membrane with excellent decoloration efficiency and antifouling performance. Journal of Membrane Science, 2022, 641, 119925.	8.2	101
46	Novel insights into membrane fouling in a membrane bioreactor: Elucidating interfacial interactions with real membrane surface. Chemosphere, 2018, 210, 769-778.	8.2	97
47	Effects of molecular weight distribution of soluble microbial products (SMPs) on membrane fouling in a membrane bioreactor (MBR): Novel mechanistic insights. Chemosphere, 2020, 248, 126013.	8.2	97
48	Enhanced visible-light-driven photocatalysis from WS <sub>2</sub> quantum dots coupled to BiOCl nanosheets: synergistic effect and mechanism insight. Catalysis Science and Technology, 2018, 8, 201-209.	4.1	95
49	Plant polyphenol intermediated metal-organic framework (MOF) membranes for efficient desalination. Journal of Membrane Science, 2021, 618, 118726.	8.2	94
50	New insights into bisphenols removal by nitrogen-rich nanocarbons: Synergistic effect between adsorption and oxidative degradation. Journal of Hazardous Materials, 2018, 345, 123-130.	12.4	93
51	Giant enhancement of photocatalytic H2 production over KNbO3 photocatalyst obtained via carbon doping and MoS2 decoration. International Journal of Hydrogen Energy, 2018, 43, 4347-4354.	7.1	91
52	A novel strategy based on magnetic field assisted preparation of magnetic and photocatalytic membranes with improved performance. Journal of Membrane Science, 2020, 612, 118378.	8.2	90
53	Novel membranes with extremely high permeability fabricated by 3D printing and nickel coating for oil/water separation. Journal of Materials Chemistry A, 2022, 10, 12055-12061.	10.3	89
54	Facile synthesis of Fe3O4-graphene@mesoporous SiO2 nanocomposites for efficient removal of Methylene Blue. Applied Surface Science, 2016, 378, 80-86.	6.1	88

#	Article	IF	CITATIONS
55	Manipulating the mussel-inspired co-deposition of tannic acid and amine for fabrication of nanofiltration membranes with an enhanced separation performance. Journal of Colloid and Interface Science, 2020, 565, 23-34.	9.4	87
56	Quantification of interfacial energies associated with membrane fouling in a membrane bioreactor by using BP and GRNN artificial neural networks. Journal of Colloid and Interface Science, 2020, 565, 1-10.	9.4	86
57	Stacking Engineering of Semiconductor Heterojunctions on Hollow Carbon Spheres for Boosting Photocatalytic CO <sub>2</sub> Reduction. ACS Catalysis, 2022, 12, 2569-2580.	11.2	86
58	Thermodynamic analysis of membrane fouling in a submerged membrane bioreactor and its implications. Bioresource Technology, 2013, 146, 7-14.	9.6	83
59	Novel conductive membranes breaking through the selectivity-permeability trade-off for Congo red removal. Separation and Purification Technology, 2019, 211, 368-376.	7.9	82
60	Surface modification of polyvinylidene fluoride (PVDF) membrane via radiation grafting: novel mechanisms underlying the interesting enhanced membrane performance. Scientific Reports, 2017, 7, 2721.	3.3	80
61	Membrane fouling by alginate in polyaluminum chloride (PACl) coagulation/microfiltration process: Molecular insights. Separation and Purification Technology, 2020, 236, 116294.	7.9	79
62	Identification of heavy metal ions from aqueous environment through gold, Silver and Copper Nanoparticles: An excellent colorimetric approach. Environmental Research, 2022, 205, 112475.	7.5	79
63	Synthesis, characterization and photocatalytic activity of visible-light plasmonic photocatalyst AgBr-SmVO4. Applied Catalysis B: Environmental, 2013, 138-139, 95-103.	20.2	78
64	Mechanisms of arsenic disruption on gonadal, adrenal and thyroid endocrine systems in humans: A review. Environment International, 2016, 95, 61-68.	10.0	78
65	Realization of quantifying interfacial interactions between a randomly rough membrane surface and a foulant particle. Bioresource Technology, 2017, 226, 220-228.	9.6	77
66	Effects of surface morphology on alginate adhesion: Molecular insights into membrane fouling based on XDLVO and DFT analysis. Chemosphere, 2019, 233, 373-380.	8.2	76
67	Mechanism analyses of high specific filtration resistance of gel and roles of gel elasticity related with membrane fouling in a membrane bioreactor. Bioresource Technology, 2018, 257, 39-46.	9.6	75
68	Application of radial basis function artificial neural network to quantify interfacial energies related to membrane fouling in a membrane bioreactor. Bioresource Technology, 2019, 293, 122103.	9.6	74
69	Radial basis function artificial neural network (RBF ANN) as well as the hybrid method of RBF ANN and grey relational analysis able to well predict trihalomethanes levels in tap water. Journal of Hydrology, 2020, 591, 125574.	5.4	74
70	Polymeric Membranes Incorporated With ZnO Nanoparticles for Membrane Fouling Mitigation: A Brief Review. Frontiers in Chemistry, 2020, 8, 224.	3.6	74
71	Impact of resuscitation promoting factor (Rpf) in membrane bioreactor treating high-saline phenolic wastewater: Performance robustness and Rpf-responsive bacterial populations. Chemical Engineering Journal, 2019, 357, 715-723.	12.7	73
72	New insights into membrane fouling by alginate: Impacts of ionic strength in presence of calcium ions. Chemosphere, 2020, 246, 125801.	8.2	73

#	Article	IF	CITATIONS
73	Facile fabrication of superhydrophilic nanofiltration membranes via tannic acid and irons layer-by-layer self-assembly for dye separation. Applied Surface Science, 2020, 515, 146063.	6.1	73
74	Electric field endowing the conductive polyvinylidene fluoride (PVDF)-graphene oxide (GO)‑nickel (Ni) membrane with high-efficient performance for dye wastewater treatment. Applied Surface Science, 2019, 483, 1006-1016.	6.1	72
75	Flame-retardant ethylene vinyl acetate composite materials by combining additions of aluminum hydroxide and melamine cyanurate: Preparation and characteristic evaluations. Journal of Colloid and Interface Science, 2021, 589, 525-531.	9.4	72
76	Thermodynamic mechanisms of membrane fouling during filtration of alginate solution in coagulation-ultrafiltration (UF) process in presence of different ionic strength and iron(III) ion concentration. Journal of Membrane Science, 2021, 635, 119532.	8.2	72
77	Electroless Ni–Sn–P plating to fabricate nickel alloy coated polypropylene membrane with enhanced performance. Journal of Membrane Science, 2021, 640, 119820.	8.2	72
78	Inkjet printing assisted fabrication of polyphenol-based coating membranes for oil/water separation. Chemosphere, 2020, 250, 126236.	8.2	71
79	Quantification of interfacial interactions between a rough sludge floc and membrane surface in a membrane bioreactor. Journal of Colloid and Interface Science, 2017, 490, 710-718.	9.4	69
80	Radial basis function artificial neural network able to accurately predict disinfection by-product levels in tap water: Taking haloacetic acids as a case study. Chemosphere, 2020, 248, 125999.	8.2	69
81	Sustainable biodegradation of phenol by immobilized Bacillus sp. SAS19 with porous carbonaceous gels as carriers. Journal of Environmental Management, 2018, 222, 185-189.	7.8	68
82	A novel strategy to develop antifouling and antibacterial conductive Cu/polydopamine/polyvinylidene fluoride membranes for water treatment. Journal of Colloid and Interface Science, 2018, 531, 493-501.	9.4	68
83	Enhanced catalytic degradation of bisphenol A by hemin-MOFs supported on boron nitride via the photo-assisted heterogeneous activation of persulfate. Separation and Purification Technology, 2019, 229, 115822.	7.9	68
84	Facile preparation of polyvinylidene fluoride substrate supported thin film composite polyamide nanofiltration: Effect of substrate pore size. Journal of Membrane Science, 2021, 638, 119699.	8.2	68
85	Novel Ternary MoS <sub>2</sub> /C-ZnO Composite with Efficient Performance in Photocatalytic NH <sub>3</sub> Synthesis under Simulated Sunlight. ACS Sustainable Chemistry and Engineering, 2018, 6, 14866-14879.	6.7	67
86	A new method for modeling rough membrane surface and calculation of interfacial interactions. Bioresource Technology, 2016, 200, 451-457.	9.6	66
87	1H-NMR based metabonomic profiling of human esophageal cancer tissue. Molecular Cancer, 2013, 12, 25.	19.2	65
88	Novel insights into membrane fouling caused by gel layer in a membrane bioreactor: Effects of hydrogen bonding. Bioresource Technology, 2019, 276, 219-225.	9.6	65
89	Facile preparation of recyclable magnetic Ni@filter paper composite materials for efficient photocatalytic degradation of methyl orange. Journal of Colloid and Interface Science, 2021, 582, 291-300.	9.4	65
90	A novel composite membrane for simultaneous separation and catalytic degradation of oil/water emulsion with high performance. Chemosphere, 2022, 288, 132490.	8.2	65

#	Article	IF	CITATIONS
91	Molecular insights into the impacts of iron(III) ions on membrane fouling by alginate. Chemosphere, 2020, 242, 125232.	8.2	64
92	Inkjet printing assisted electroless Ni plating to fabricate nickel coated polypropylene membrane with improved performance. Journal of Colloid and Interface Science, 2020, 565, 546-554.	9.4	64
93	Insight into the mechanisms for hexavalent chromium reduction and sulfisoxazole degradation catalyzed by graphitic carbon nitride: The Yin and Yang in the photo-assisted processes. Chemosphere, 2019, 221, 166-174.	8.2	63
94	Mo-doped Co3O4 ultrathin nanosheet arrays anchored on nickel foam as a bi-functional electrode for supercapacitor and overall water splitting. Journal of Colloid and Interface Science, 2021, 602, 355-366.	9.4	61
95	Novel in-situ electroflotation driven by hydrogen evolution reaction (HER) with polypyrrole (PPy)-Ni-modified fabric membrane for efficient oil/water separation. Journal of Membrane Science, 2021, 635, 119502.	8.2	60
96	Synthesis of KNbO3/g-C3N4 composite and its new application in photocatalytic H2 generation under visible light irradiation. Journal of Materials Science, 2018, 53, 7453-7465.	3.7	57
97	Enzyme-mimicking single-atom FeN4 sites for enhanced photo-Fenton-like reactions. Applied Catalysis B: Environmental, 2022, 310, 121327.	20.2	57
98	Physicochemical correlations between membrane surface hydrophilicity and adhesive fouling in membrane bioreactors. Journal of Colloid and Interface Science, 2017, 505, 900-909.	9.4	56
99	Bamboo-like carbon nanotubes derived from colloidal polymer nanoplates for efficient removal of bisphenol A. Journal of Materials Chemistry A, 2016, 4, 15450-15456.	10.3	55
100	Filtration behaviors and fouling mechanisms of ultrafiltration process with polyacrylamide flocculation for water treatment. Science of the Total Environment, 2020, 703, 135540.	8.0	55
101	In-situ coating TiO2 surface by plant-inspired tannic acid for fabrication of thin film nanocomposite nanofiltration membranes toward enhanced separation and antibacterial performance. Journal of Colloid and Interface Science, 2020, 572, 114-121.	9.4	55
102	Enhancement of polychlorinated biphenyl biodegradation by resuscitation promoting factor (Rpf) and Rpf-responsive bacterial community. Chemosphere, 2021, 263, 128283.	8.2	55
103	Bacterial community shifts evaluation in the sediments of Puyang River and its nitrogen removal capabilities exploration by resuscitation promoting factor. Ecotoxicology and Environmental Safety, 2019, 179, 188-197.	6.0	54
104	Enhanced visible-light photoactivity of g-C3N4 via Zn2SnO4 modification. Applied Surface Science, 2015, 329, 143-149.	6.1	53
105	Biocompatible G-Fe3O4/CA nanocomposites for the removal of Methylene Blue. Journal of Molecular Liquids, 2015, 212, 63-69.	4.9	53
106	Membrane fouling in a membrane bioreactor: A novel method for membrane surface morphology construction and its application in interaction energy assessment. Journal of Membrane Science, 2016, 516, 135-143.	8.2	53
107	Factors influencing DBPs occurrence in tap water of Jinhua Region in Zhejiang Province, China. Ecotoxicology and Environmental Safety, 2019, 171, 813-822.	6.0	53
108	Magnetic field assisted preparation of PES-Ni@MWCNTs membrane with enhanced permeability and antifouling performance. Chemosphere, 2020, 243, 125446.	8.2	53

#	Article	IF	CITATIONS
109	A facile method for simulating randomly rough membrane surface associated with interface behaviors. Applied Surface Science, 2018, 427, 915-921.	6.1	52
110	Using simple and easy water quality parameters to predict trihalomethane occurrence in tap water. Chemosphere, 2022, 286, 131586.	8.2	52
111	Preparation of nickel@polyvinyl alcohol (PVA) conductive membranes to couple a novel electrocoagulation-membrane separation system for efficient oil-water separation. Journal of Membrane Science, 2022, 653, 120541.	8.2	52
112	Novel platinum-bismuth alloy loaded KTa0.5Nb0.5O3 composite photocatalyst for effective nitrogen-to-ammonium conversion. Journal of Colloid and Interface Science, 2022, 618, 362-374.	9.4	51
113	Membrane technologies for microalgal cultivation and dewatering: Recent progress and challenges. Algal Research, 2019, 44, 101686.	4.6	49
114	Pesticide residues in breast milk and the associated risk assessment: A review focused on China. Science of the Total Environment, 2020, 727, 138412.	8.0	49
115	Novel catalytic self-cleaning membrane with peroxymonosulfate activation for dual-function wastewater purification: Performance and mechanism. Journal of Cleaner Production, 2022, 355, 131858.	9.3	49
116	The biological performance of a novel microalgal-bacterial membrane photobioreactor: Effects of HRT and N/P ratio. Chemosphere, 2020, 261, 128199.	8.2	48
117	Simultaneous determination of dopamine and uric acid using layer-by-layer graphene and chitosan assembled multilayer films. Talanta, 2013, 117, 359-365.	5.5	47
118	Resuscitation of functional bacterial community for enhancing biodegradation of phenol under high salinity conditions based on Rpf. Bioresource Technology, 2018, 261, 394-402.	9.6	47
119	Improved thermal stability and heat-aging resistance of silicone rubber via incorporation of UiO-66-NH2. Materials Chemistry and Physics, 2021, 274, 125182.	4.0	47
120	Surface Properties of Biofouled Membranes from a Submerged Anaerobic Membrane Bioreactor after Cleaning. Journal of Environmental Engineering, ASCE, 2011, 137, 504-513.	1.4	46
121	Enhanced performance of a submerged membrane bioreactor with powdered activated carbon addition for municipal secondary effluent treatment. Journal of Hazardous Materials, 2011, 192, 1509-1514.	12.4	46
122	Organic dye doped graphitic carbon nitride with a tailored electronic structure for enhanced photocatalytic hydrogen production. Catalysis Science and Technology, 2019, 9, 502-508.	4.1	45
123	Fabrication of hydrophilic and antibacterial poly(vinylidene fluoride) based separation membranes by a novel strategy combining radiation grafting of poly(acrylic acid) (PAA) and electroless nickel plating. Journal of Colloid and Interface Science, 2019, 543, 64-75.	9.4	45
124	Viable but Nonculturable State of Yeast <i>Candida</i> sp. Strain LN1 Induced by High Phenol Concentrations. Applied and Environmental Microbiology, 2021, 87, e0111021.	3.1	45
125	Fundamental thermodynamic mechanisms of membrane fouling caused by transparent exopolymer particles (TEP) in water treatment. Science of the Total Environment, 2022, 820, 153252.	8.0	45
126	Membrane fouling in a submerged membrane bioreactor: Effect of pH and its implications. Bioresource Technology, 2014, 152, 7-14.	9.6	44

#	Article	IF	CITATIONS
127	Influence of membrane surface roughness on interfacial interactions with sludge flocs in a submerged membrane bioreactor. Journal of Colloid and Interface Science, 2015, 446, 84-90.	9.4	44
128	Precursors for brominated haloacetic acids during chlorination and a new useful indicator for bromine substitution factor. Science of the Total Environment, 2020, 698, 134250.	8.0	44
129	Osmotic pressure effect on membrane fouling in a submerged anaerobic membrane bioreactor and its experimental verification. Bioresource Technology, 2012, 125, 97-101.	9.6	43
130	Novel indicators for thermodynamic prediction of interfacial interactions related with adhesive fouling in a membrane bioreactor. Journal of Colloid and Interface Science, 2017, 487, 320-329.	9.4	43
131	Preparation, characterization, and photocatalytic activity of novel AgBr/ZIF-8 composites for water purification. Advanced Powder Technology, 2020, 31, 439-447.	4.1	43
132	<i>In situ</i> conversion of ZnO into zeolitic imidazolate framework-8 in polyamide layers for well-structured high-permeance thin-film nanocomposite nanofiltration membranes. Journal of Materials Chemistry A, 2021, 9, 7684-7691.	10.3	43
133	A new strategy to accelerate co-deposition of plant polyphenol and amine for fabrication of antibacterial nanofiltration membranes by in-situ grown Ag nanoparticles. Separation and Purification Technology, 2022, 280, 119866.	7.9	43
134	Photodegradation of RhB over YVO4/g-C3N4 composites under visible light irradiation. RSC Advances, 2013, 3, 20862.	3.6	42
135	Thermophilic membrane bioreactors: A review. Bioresource Technology, 2017, 243, 1180-1193.	9.6	42
136	Developing predictive models for toxicity of organic chemicals to green algae based on mode of action. Chemosphere, 2018, 190, 463-470.	8.2	42
137	Effective partial denitrification of biological effluent of landfill leachate for Anammox process: Start-up, influencing factors and stable operation. Science of the Total Environment, 2022, 807, 150975.	8.0	42
138	Facile preparation of Ag2S/KTa0.5Nb0.5O3 heterojunction for enhanced performance in catalytic nitrogen fixation via photocatalysis and piezo-photocatalysis. Green Energy and Environment, 2023, 8, 1630-1643.	8.7	42
139	Effects of polysaccharides' molecular structure on membrane fouling and the related mechanisms. Science of the Total Environment, 2022, 836, 155579.	8.0	41
140	Synthesis, characterization and photocatalytic performance of VDyO composite under visible light irradiation. Chemical Engineering Journal, 2011, 169, 50-57.	12.7	40
141	Pollutant removal and membrane fouling in an anaerobic submerged membrane bioreactor for real sewage treatment. Water Science and Technology, 2014, 69, 1712-1719.	2.5	40
142	Aerobic degradation of 3,3′,4,4′-tetrachlorobiphenyl by a resuscitated strain Castellaniella sp. SPC4: Kinetics model and pathway for biodegradation. Science of the Total Environment, 2019, 688, 917-925.	8.0	40
143	The toxicity of 2,6-dichlorobenzoquinone on the early life stage of zebrafish: A survey on the endpoints at developmental toxicity, oxidative stress, genotoxicity and cytotoxicity. Environmental Pollution, 2019, 245, 719-724.	7.5	40
144	Use of multiple regression models to evaluate the formation of halonitromethane via chlorination/chloramination of water from Tai Lake and the Qiantang River, China. Chemosphere, 2015, 119, 540-546.	8.2	39

#	Article	IF	CITATIONS
145	Effects of surface charge on interfacial interactions related to membrane fouling in a submerged membrane bioreactor based on thermodynamic analysis. Journal of Colloid and Interface Science, 2016, 465, 33-41.	9.4	39
146	Bromine incorporation into five DBP classes upon chlorination of water with extremely low SUVA values. Science of the Total Environment, 2017, 590-591, 720-728.	8.0	39
147	A comparative study on the photocatalytic activities of two visible-light plasmonic photocatalysts: AgCl-SmVO4 and AgI-SmVO4 composites. Applied Catalysis A: General, 2014, 472, 143-151.	4.3	38
148	Fabrication, characterization and photocatalytic activity of g-C <sub>3</sub> N <sub>4</sub> coupled with FeVO <sub>4</sub> nanorods. RSC Advances, 2015, 5, 27933-27939.	3.6	38
149	Mechanistic insights into Ca-alginate gel-associated membrane fouling affected by ethylene diamine tetraacetic acid (EDTA). Science of the Total Environment, 2022, 842, 156912.	8.0	38
150	Fractal reconstruction of rough membrane surface related with membrane fouling in a membrane bioreactor. Bioresource Technology, 2016, 216, 817-823.	9.6	37
151	Formation of disinfection by-products during chlorination of organic matter from phoenix tree leaves and Chlorella vulgaris. Environmental Pollution, 2018, 243, 1887-1893.	7.5	37
152	Membrane fouling in a submerged membrane bioreactor: New method and its applications in interfacial interaction quantification. Bioresource Technology, 2017, 241, 406-414.	9.6	36
153	Whole-genome sequencing of an acidophilic Rhodotorula sp. ZM1 and its phenol-degrading capability under acidic conditions. Chemosphere, 2019, 232, 76-86.	8.2	36
154	Effects of ionic strength on membrane fouling in a membrane bioreactor. Bioresource Technology, 2014, 156, 35-41.	9.6	35
155	Regression models evaluating THMs, HAAs and HANs formation upon chloramination of source water collected from Yangtze River Delta Region, China. Ecotoxicology and Environmental Safety, 2018, 160, 249-256.	6.0	35
156	A facile method to modify polypropylene membrane by polydopamine coating via inkjet printing technique for superior performance. Journal of Colloid and Interface Science, 2019, 552, 719-727.	9.4	34
157	Significantly Enhanced Photocatalytic CO <sub>2</sub> Reduction by Surface Amorphization of Cocatalysts. Small, 2021, 17, e2102105.	10.0	34
158	Facile large scale fabrication of magnetic carbon nano-onions for efficient removal of bisphenol A. Materials Chemistry and Physics, 2017, 198, 186-192.	4.0	33
159	Novel carbon modified KTa0.75Nb0.25O3 nanocubes with excellent efficiency in photocatalytic H2 evolution. Fuel, 2018, 233, 486-496.	6.4	33
160	Resuscitation of viable but nonâ€culturable bacteria to enhance the celluloseâ€degrading capability of bacterial community in composting. Microbial Biotechnology, 2018, 11, 527-536.	4.2	32
161	New strategy of grafting hydroxyethyl acrylate (HEA) via Î <sup>3</sup> ray radiation to modify polyvinylidene fluoride (PVDF) membrane: Thermodynamic mechanisms of the improved antifouling performance. Separation and Purification Technology, 2018, 207, 83-91.	7.9	32
162	Plant polyphenols induced the synthesis of rich oxygen vacancies Co3O4/Co@N-doped carbon hollow nanomaterials for electrochemical energy storage and conversion. Journal of Colloid and Interface Science, 2021, 600, 58-71.	9.4	32

#	Article	IF	CITATIONS
163	Ultrasound-assisted catalytic activation of peroxydisulfate on Ti3GeC2 MAX phase for efficient removal of hazardous pollutants. Materials Today Chemistry, 2022, 24, 100818.	3.5	32
164	A novel approach for quantitative evaluation of the physicochemical interactions between rough membrane surface and sludge foulants in a submerged membrane bioreactor. Bioresource Technology, 2014, 171, 247-252.	9.6	31
165	YLT192, a Novel, Orally Active Bioavailable Inhibitor of VEGFR2 Signaling with Potent Antiangiogenic Activity and Antitumor Efficacy in Preclinical Models. Scientific Reports, 2015, 4, 6031.	3.3	31
166	A novel insight into membrane fouling mechanism regarding gel layer filtration: Flory-Huggins based filtration mechanism. Scientific Reports, 2016, 6, 33343.	3.3	31
167	Effects of fractal roughness of membrane surfaces on interfacial interactions associated with membrane fouling in a membrane bioreactor. Bioresource Technology, 2017, 244, 560-568.	9.6	31
168	Semi-sacrificial template synthesis of single-atom Ni sites supported on hollow carbon nanospheres for efficient and stable electrochemical CO <sub>2</sub> reduction. Inorganic Chemistry Frontiers, 2020, 7, 1719-1725.	6.0	31
169	Camptothecin nanocolloids based on N,N,N-trimethyl chitosan: Efficient suppression of growth of multiple myeloma in a murine model. Oncology Reports, 2012, 27, 1035-1040.	2.6	30
170	Using regression models to evaluate the formation of trihalomethanes and haloacetonitriles via chlorination of source water with low SUVA values in the Yangtze River Delta region, China. Environmental Geochemistry and Health, 2016, 38, 1303-1312.	3.4	30
171	Thermodynamic analysis of effects of contact angle on interfacial interactions and its implications for membrane fouling control. Bioresource Technology, 2016, 201, 245-252.	9.6	30
172	Effectively H2 generation over CdS/KTa0.75Nb0.25O3 composite via water splitting. Journal of Colloid and Interface Science, 2019, 552, 622-632.	9.4	30
173	Environmentally relevant concentrations of arsenite induces developmental toxicity and oxidative responses in the early life stage of zebrafish. Environmental Pollution, 2019, 254, 113022.	7.5	29
174	Effective decolorization of anthraquinone dye reactive blue 19 using immobilized Bacillus sp. JF4 isolated by resuscitation-promoting factor strategy. Water Science and Technology, 2020, 81, 1159-1169.	2.5	29
175	Pressure-assisted polydopamine modification of thin-film composite reverse osmosis membranes for enhanced desalination and antifouling performance. Desalination, 2022, 530, 115671.	8.2	29
176	Influences of fractal dimension of membrane surface on interfacial interactions related to membrane fouling in a membrane bioreactor. Journal of Colloid and Interface Science, 2017, 500, 79-87.	9.4	28
177	Membrane fouling in a submerged membrane bioreactor with focus on surface properties and interactions of cake sludge and bulk sludge. Bioresource Technology, 2014, 169, 213-219.	9.6	27
178	Ultrathin graphene layer activated dendritic α-Fe2O3 for high performance asymmetric supercapacitors. Journal of Alloys and Compounds, 2019, 780, 212-219.	5.5	26
179	Novel molecular level insights into forward osmosis membrane fouling affected by reverse diffusion of draw solutions based on thermodynamic mechanisms. Journal of Membrane Science, 2021, 620, 118815.	8.2	25
180	Effect of nitrite on the formation of halonitromethanes during chlorination of organic matter from different origin. Journal of Hydrology, 2015, 531, 802-809.	5.4	24

#	Article	IF	CITATIONS
181	Effects of molecular weight distribution (Md) on the performances of the polyethersulfone (PES) ultrafiltration membranes. Journal of Membrane Science, 2015, 490, 220-226.	8.2	24
182	Modeling three-dimensional surface morphology of biocake layer in a membrane bioreactor based on fractal geometry. Bioresource Technology, 2016, 222, 478-484.	9.6	24
183	A novel integrated method for quantification of interfacial interactions between two rough bioparticles. Journal of Colloid and Interface Science, 2018, 516, 295-303.	9.4	24
184	Facile preparation of polyacrylonitrile-co-methylacrylate based integrally skinned asymmetric nanofiltration membranes for sustainable molecular separation: An one-step method. Journal of Colloid and Interface Science, 2019, 546, 251-261.	9.4	24
185	Preparation and characterization of ethylene–vinyl acetate copolymer (EVA)–magnesium hydroxide (MH)–hexaphenoxycyclotriphosphazene (HPCTP) composite flame-retardant materials. Polymer Bulletin, 2019, 76, 2399-2410.	3.3	24
186	The promising NIR light-driven MO3-x (MÂ=ÂMo, W) photocatalysts for energy conversion and environmental remediation. Chemical Engineering Journal, 2022, 431, 134044.	12.7	24
187	Influences of acid–base property of membrane on interfacial interactions related with membrane fouling in a membrane bioreactor based on thermodynamic assessment. Bioresource Technology, 2016, 214, 355-362.	9.6	23
188	Quantitative assessment of interfacial forces between two rough surfaces and its implications for anti-adhesion membrane fabrication. Separation and Purification Technology, 2017, 189, 238-245.	7.9	23
189	What is the better choice for Pd cocatalysts for photocatalytic reduction of CO <sub>2</sub> to renewable fuels: high-crystallinity or amorphous?. Journal of Materials Chemistry A, 2020, 8, 21208-21218.	10.3	23
190	Preparation and Characterization of Ag‣oaded Sm <scp><scp>VO</scp></scp> <sub>4</sub> for Photocatalysis Application. Photochemistry and Photobiology, 2013, 89, 529-535.	2.5	22
191	Experimental evidence for osmotic pressure-induced fouling in a membrane bioreactor. Bioresource Technology, 2014, 158, 119-126.	9.6	22
192	<i>In Silico</i> Investigation of the Thyroid Hormone Activity of Hydroxylated Polybrominated Diphenyl Ethers. Chemical Research in Toxicology, 2015, 28, 1538-1545.	3.3	22
193	Magnetic ZnFe <sub>2</sub> O <sub>4</sub> @chitosan encapsulated in graphene oxide for adsorptive removal of organic dye. RSC Advances, 2017, 7, 28145-28151.	3.6	22
194	A New Approach of Rpf Addition to Explore Bacterial Consortium for Enhanced Phenol Degradation Under High Salinity Conditions. Current Microbiology, 2018, 75, 1046-1054.	2.2	22
195	A new strategy to produce low-density polyethylene (LDPE)-based composites simultaneously with high flame retardancy and high mechanical properties. Applied Surface Science, 2018, 437, 75-81.	6.1	22
196	Thermodynamic assessment of adsorptive fouling with the membranes modified via layer-by-layer self-assembly technique. Journal of Colloid and Interface Science, 2017, 494, 194-203.	9.4	21
197	Graphynes: ideal supports of single atoms for electrochemical energy conversion. Journal of Materials Chemistry A, 2022, 10, 3905-3932.	10.3	21
198	Thiophene insertion and lanthanum molybdate modification of g-C3N4 for enhanced visible-light-driven photoactivity in tetracycline degradation. Applied Surface Science, 2022, 592, 153337.	6.1	21

#	Article	IF	CITATIONS
199	A new approach to construct three-dimensional surface morphology of sludge flocs in a membrane bioreactor. Bioresource Technology, 2016, 219, 521-526.	9.6	20
200	A facile strategy to prepare superhydrophilic polyvinylidene fluoride (PVDF) based membranes and the thermodynamic mechanisms underlying the improved performance. Separation and Purification Technology, 2018, 197, 271-280.	7.9	20
201	Rationally designed Ni <sub>2</sub> P/Ni/C as a positive electrode for high-performance hybrid supercapacitors. New Journal of Chemistry, 2020, 44, 6810-6817.	2.8	20
202	Quantitative evaluation of the interfacial interactions between a randomly rough sludge floc and membrane surface in a membrane bioreactor based on fractal geometry. Bioresource Technology, 2017, 234, 198-207.	9.6	19
203	Layered Co doped MnO2 with abundant oxygen defects to boost aqueous zinc-ion storage. Journal of Colloid and Interface Science, 2022, 611, 662-669.	9.4	19
204	Quantitative assessment of interfacial interactions with rough membrane surface and its implications for membrane selection and fabrication in a MBR. Bioresource Technology, 2015, 179, 367-372.	9.6	18
205	Tuning anti-adhesion ability of membrane for a membrane bioreactor by thermodynamic analysis. Bioresource Technology, 2016, 216, 691-698.	9.6	18
206	Characterization of foaming and non-foaming sludge relating to aeration and the implications for membrane fouling control in submerged membrane bioreactors. Journal of Water Process Engineering, 2019, 28, 250-259.	5.6	18
207	Pesticides in human milk collected from Jinhua, China: Levels, influencing factors and health risk assessment. Ecotoxicology and Environmental Safety, 2020, 205, 111331.	6.0	18
208	Simultaneously improving mechanical strength, hydrophobic property and flame retardancy of ethylene vinyl acetate copolymer/intumescent flame retardant/FeOOH by introducing modified fumed silica. Materials Today Communications, 2021, 26, 102114.	1.9	18
209	New Application and Excellent Performance of Ag/KNbO <sub>3</sub> Nanocomposite in Photocatalytic NH <sub>3</sub> Synthesis. ACS Sustainable Chemistry and Engineering, 0, , .	6.7	17
210	Cyclophosphamide induced physiological and biochemical changes in mice with an emphasis on sensitivity analysis. Ecotoxicology and Environmental Safety, 2021, 211, 111889.	6.0	17
211	A biobased flame retardant towards improvement of flame retardancy and mechanical property of ethylene vinyl acetate. Chinese Chemical Letters, 2023, 34, 107202.	9.0	17
212	Preparation, characterization, and photocatalytic activity of CdV2O6 nanorods decorated g-C3N4 composite. Journal of Molecular Catalysis A, 2016, 423, 240-247.	4.8	16
213	Dual active sites of the Co <sub>2</sub> N and single-atom Co–N <sub>4</sub> embedded in nitrogen-rich nanocarbons: a robust electrocatalyst for oxygen reduction reactions. Nanotechnology, 2020, 31, 165401.	2.6	16
214	Effective biological nitrogen process and nitrous oxide emission characteristics for the treatment of landfill leachate with low carbon-to-nitrogen ratio. Journal of Cleaner Production, 2020, 268, 122289.	9.3	16
215	<scp>YL529</scp> , a novel, orally available multikinase inhibitor, potently inhibits angiogenesis and tumour growth in preclinical models. British Journal of Pharmacology, 2013, 169, 1766-1780.	5.4	15
216	Chronic exposure to dichloroacetamide induces biochemical and histopathological changes in the gills of zebrafish. Environmental Toxicology, 2019, 34, 781-787.	4.0	15

#	Article	IF	CITATIONS
217	Membrane fouling in a microalgal-bacterial membrane photobioreactor: Effects of P-availability controlled by N:P ratio. Chemosphere, 2021, 282, 131015.	8.2	15
218	Evaluation of membrane fouling in a microalgal-bacterial membrane photobioreactor: Effects of SRT. Science of the Total Environment, 2022, 839, 156414.	8.0	15
219	Modeling and predicting pKa values of mono-hydroxylated polychlorinated biphenyls (HO-PCBs) and polybrominated diphenyl ethers (HO-PBDEs) by local molecular descriptors. Chemosphere, 2015, 138, 829-836.	8.2	14
220	Simulation of foulant bioparticle topography based on Gaussian process and its implications for interface behavior research. Applied Surface Science, 2018, 434, 975-981.	6.1	13
221	In-situ growth of UiO-66-NH2 in porous polymeric substrates at room temperature for fabrication of mixed matrix membranes with fast molecular separation performance. Chemical Engineering Journal, 2022, 435, 134804.	12.7	13
222	Molecular level insights into the dynamic evolution of forward osmosis fouling via thermodynamic modeling and quantum chemistry calculation: Effect of protein/polysaccharide ratios. Journal of Membrane Science, 2022, 655, 120588.	8.2	13
223	Current Methods and Research Progress in Nanomaterials Risk Assessment. Current Drug Metabolism, 2012, 13, 354-363.	1.2	12
224	Effects of ozone pretreatment on the formation of disinfection by-products and its associated bromine substitution factors upon chlorination/chloramination of Tai Lake water. Science of the Total Environment, 2014, 475, 23-28.	8.0	12
225	Membrane fouling in a submerged membrane bioreactor: An unified approach to construct topography and to evaluate interaction energy between two randomly rough surfaces. Bioresource Technology, 2017, 243, 1121-1132.	9.6	11
226	Effects of solids retention time on the biological performance of a novel microalgal-bacterial membrane photobioreactor for industrial wastewater treatment. Journal of Environmental Chemical Engineering, 2021, 9, 105500.	6.7	11
227	Developing QSPR model of gas/particle partition coefficients of neutral poly-/perfluoroalkyl substances. Atmospheric Environment, 2016, 143, 270-277.	4.1	10
228	The enhanced compatibility and flame retarding ability of UHMWPE-MH composites by adding phenoxycyclophosphazene (HPCTP). Polymer Bulletin, 2017, 74, 3639-3655.	3.3	10
229	Factors affecting formation of haloacetonitriles and haloketones during chlorination/monochloramination of Jinlan Reservoir water. Water Science and Technology: Water Supply, 2013, 13, 1123-1129.	2.1	9
230	Validation of a high-performance liquid chromatographic ultraviolet detection method for the quantification of vandetanib in rat plasma and its application to pharmacokinetic studies. Journal of Cancer Research and Therapeutics, 2014, 10, 84.	0.9	9
231	Adsorption of Methyl Violet Onto Mesoporous MCM-48 from Aqueous Solution. Journal of Nanoscience and Nanotechnology, 2014, 14, 4655-4663.	0.9	9
232	Preparation, characterization and photocatalytic activity of graphene doped SmVO4 photocatalyst. Materials Letters, 2014, 122, 17-20.	2.6	9
233	Impacts of morphology on fouling propensity in a membrane bioreactor based on thermodynamic analyses. Journal of Colloid and Interface Science, 2018, 531, 282-290.	9.4	9
234	Synergistic fouling behaviors and thermodynamic mechanisms of proteins and polysaccharides in forward osmosis: The unique role of reverse solute diffusion. Desalination, 2022, 536, 115850.	8.2	9

#	Article	IF	CITATIONS
235	A unified thermodynamic fouling mechanism based on forward osmosis membrane unique properties: An asymmetric structure and reverse solute diffusion. Science of the Total Environment, 2022, 808, 152219.	8.0	8
236	Membrane Photobioreactor Applied for Municipal Wastewater Treatment at a High Solids Retention Time: Effects of Microalgae Decay on Treatment Performance and Biomass Properties. Membranes, 2022, 12, 564.	3.0	8
237	Computational Insight into the Activation Mechanism of Carcinogenic <i>N</i> '-Nitrosonornicotine (NNN) Catalyzed by Cytochrome P450. Environmental Science & Technology, 2018, 52, 11838-11847.	10.0	7
238	Development and evaluation of predictive model for bovine serum albumin-water partition coefficients of neutral organic chemicals. Ecotoxicology and Environmental Safety, 2017, 138, 92-97.	6.0	6
239	Hot-pressed membrane assemblies enhancing the biofilm formation and nitrogen removal in a membrane-aerated biofilm reactor. Science of the Total Environment, 2022, 833, 155003.	8.0	6
240	Precursor characteristics of mono-HAAs during chlorination and cytotoxicity of mono-HAAs on HEK-293T cells. Chemosphere, 2022, 301, 134689.	8.2	6
241	Pharmacokinetic Studies of a Novel Multikinase Inhibitor for Treating Cancer by HPLC-UV. Journal of Chromatographic Science, 2013, 51, 17-20.	1.4	5
242	A small molecular agent YL529 inhibits VEGF-D-induced lymphangiogenesis and metastasis in preclinical tumor models in addition to its known antitumor activities. BMC Cancer, 2015, 15, 525.	2.6	5
243	Thermodynamic insights into membrane fouling in a membrane bioreactor: Evaluating thermodynamic interactions with Gaussian membrane surface. Journal of Colloid and Interface Science, 2018, 527, 280-288.	9.4	5
244	SKLB70326, a novel small-molecule inhibitor of cell-cycle progression, induces G0/G1 phase arrest and apoptosis in human hepatic carcinoma cells. Biochemical and Biophysical Research Communications, 2012, 421, 684-689.	2.1	4
245	Nitrogen Doped Nanoporous Carbon Derived from Zizania Latifolia for Adsorptive Removal of Bisphenol A. Journal of Nanoscience and Nanotechnology, 2019, 19, 1026-1034.	0.9	4
246	Author's responses to the comment by Seong-Hoon Yoon on "A new insight into membrane fouling mechanism in submerged membrane bioreactor: Osmotic pressure during cake layer filtration― published in Water Research, vol. 47, pp.Â2777–2786, 2013. Water Research, 2013, 47, 4790-4791.	11.3	3
247	The observation of <scp>PP</scp> / <scp>EVA</scp> blends in which isotactic <scp>PP</scp> was preradiated with different radiation absorbed doses. Journal of Applied Polymer Science, 2017, 134, 45057.	2.6	3
248	One-Pot and Surfactant-Free Synthesis of Ultrafine PtSn Nanoparticles Supported on Onion-Like Nanocarbons Toward Efficient Methanol and Ethylene Glycol Oxidation Reactions. Journal of Nanoscience and Nanotechnology, 2020, 20, 2408-2415.	0.9	3
249	Water-dispersible, pH- and ultralong stable, biocompatible, and highly luminescent graphite-like poly(l-proline) dots: a cytoplasm staining reagent. RSC Advances, 2014, 4, 23826.	3.6	2
250	Advanced membrane bioreactor fouling control and prevention strategies. , 2020, , 209-224.		1
251	A review on predicting p <italic>K</italic> <sub>a</sub> values of small organic compounds. Chinese Science Bulletin, 2015, 60, 1261-1271.	0.7	1
252	Effects of Van Der Waals Surface Energy on Membrane Fouling in a Submerged Membrane Bioreactor (MBR). Current Environmental Engineering, 2015, 2, 50-55.	0.6	1

#	Article	IF	CITATIONS
253	Adsorption of U(VI) by boron nitride-supported iron phosphotungstate: an experimental and mechanism study. Scientia Sinica Chimica, 2019, 49, 123-132.	0.4	0